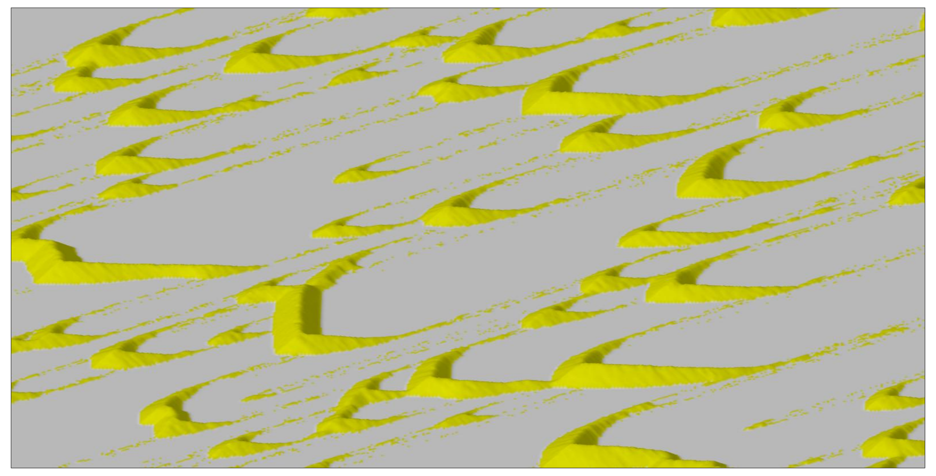

The application of automated pattern metrics to surface moisture influences on modelled dune field development

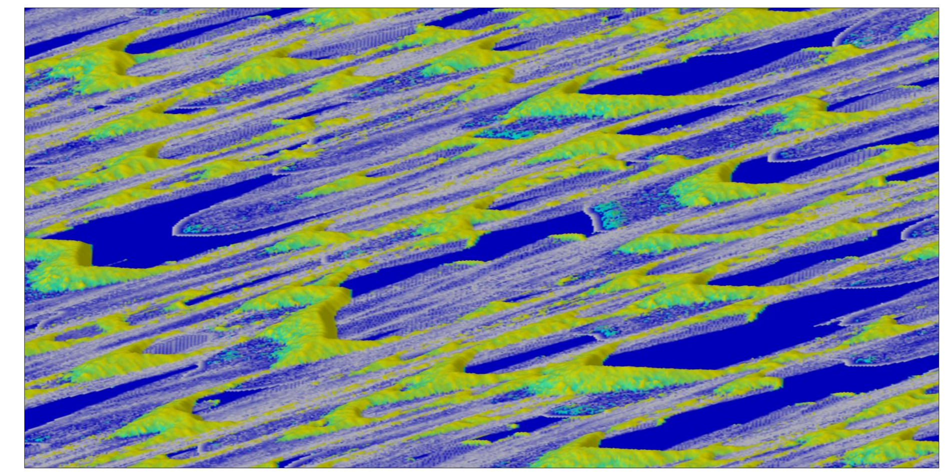

UNIVERSITY OF Southampton
School of Geography

Robin T. Wilson and Joanna M. Nield

1. Background

Aeolian dunefields develop complex patterns that are influenced by past and present environmental conditions (Ewing *et al.* 2006). Here we quantify these patterns using metrics such as average crest length, defect density and nearest neighbour R-values through an automated procedure which can be applied to Digital Elevation Models. This method offers an improvement over the manual digitisation of dune crests as it is fast and repeatable, thus allowing statistics to be easily extracted from large numbers of spatial and temporal configurations. We illustrate this method through its application to DECAL (Nield and Baas, 2008) simulations examining surface moisture influences on self-organisation pattern development. This automated method has the potential to improve our understanding of dunefield configurations, particularly as LiDAR and satellite data become increasingly available.

2. Dune Analysis Methodology

We employ a two-part automated method to extract the crests of sand dunes from a Digital Elevation Model (DEM) and calculate pattern metrics from these crests. First we extract crests from a DEM and convert these to a binary raster image. We then convert these raster crests into a series of lines in a GIS to enable pattern analysis to be performed.

Crest Extraction:

The crests are extracted using an algorithm which finds the significant change in aspect when two opposite slopes meet (for example, from an aspect < 180 to > 180). This is done by creating an aspect image from the DEM and moving across the image marking each major change in aspect as a dune crest. The simple map of crest locations which is produced is then refined by filling in the gaps between dune crests which are within on pixel of one-another. This enables a single line element to be created for each dune crest in the GIS procedure which follows. To reduce noise in the output image extremely low values in the DEM are removed, and the aspect image is smoothed with a 3 x 3 low pass filter before extraction takes place. This method is completely automated using code written in IDL using the ENVI 4.6 API.

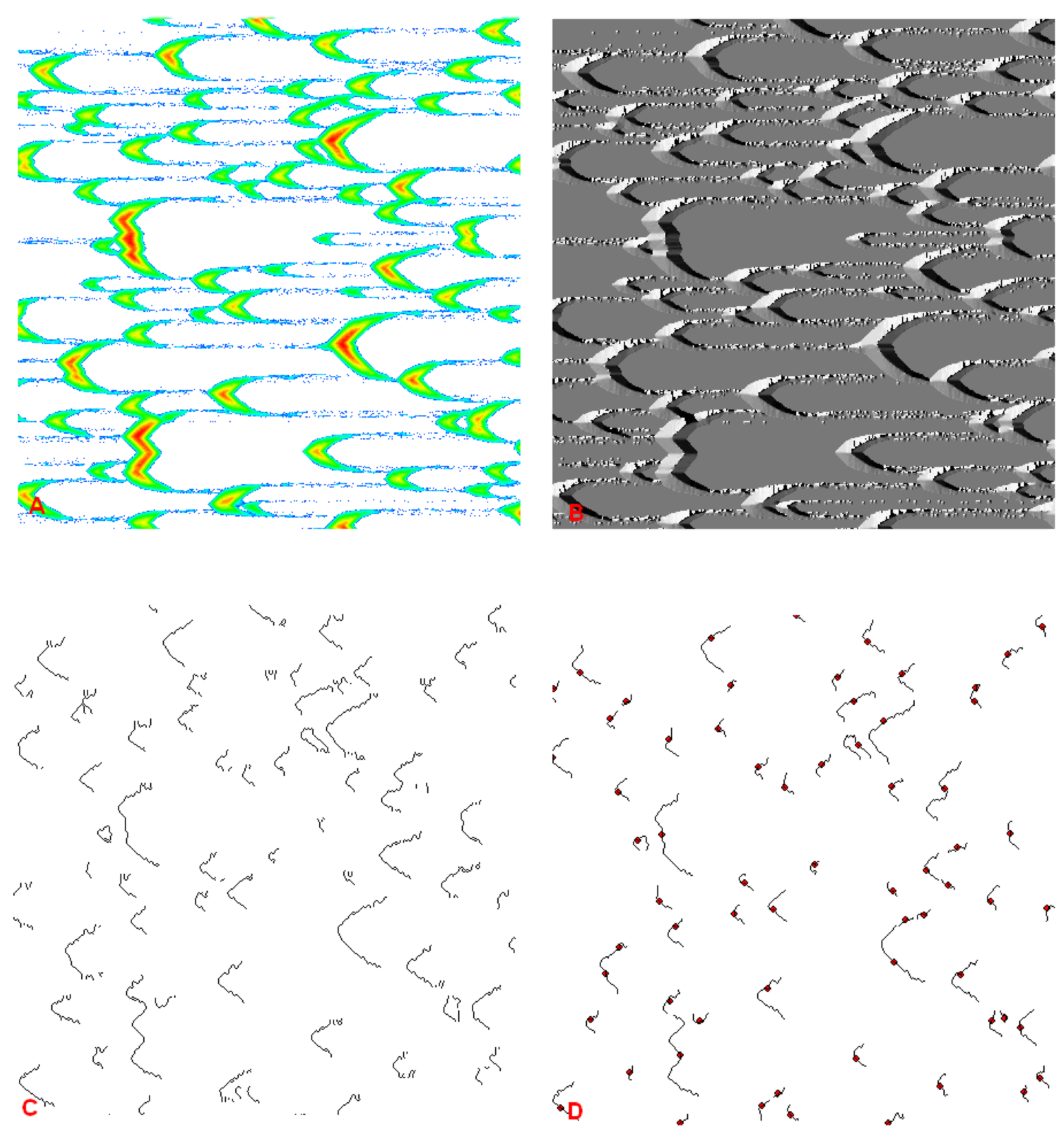

Fig. 2.1 A. example DEM, B. aspect image, C. binary crest image, D. GIS crest extraction and point insertion

GIS analysis:

The binary crest image is imported and converted to a set of polylines (using a configurable minimum length parameter). The mean, maximum and standard deviation of the line lengths are then calculated, along with the number of dunes (defined as the number of extracted lines, assuming one crest line is extracted per dune). Defect density is calculated as the number of dunes divided by the total length, and points are placed at the centre of each line (using the single point method of Wilkins and Ford (2007)) to allow the Nearest Neighbour R-score to be calculated.

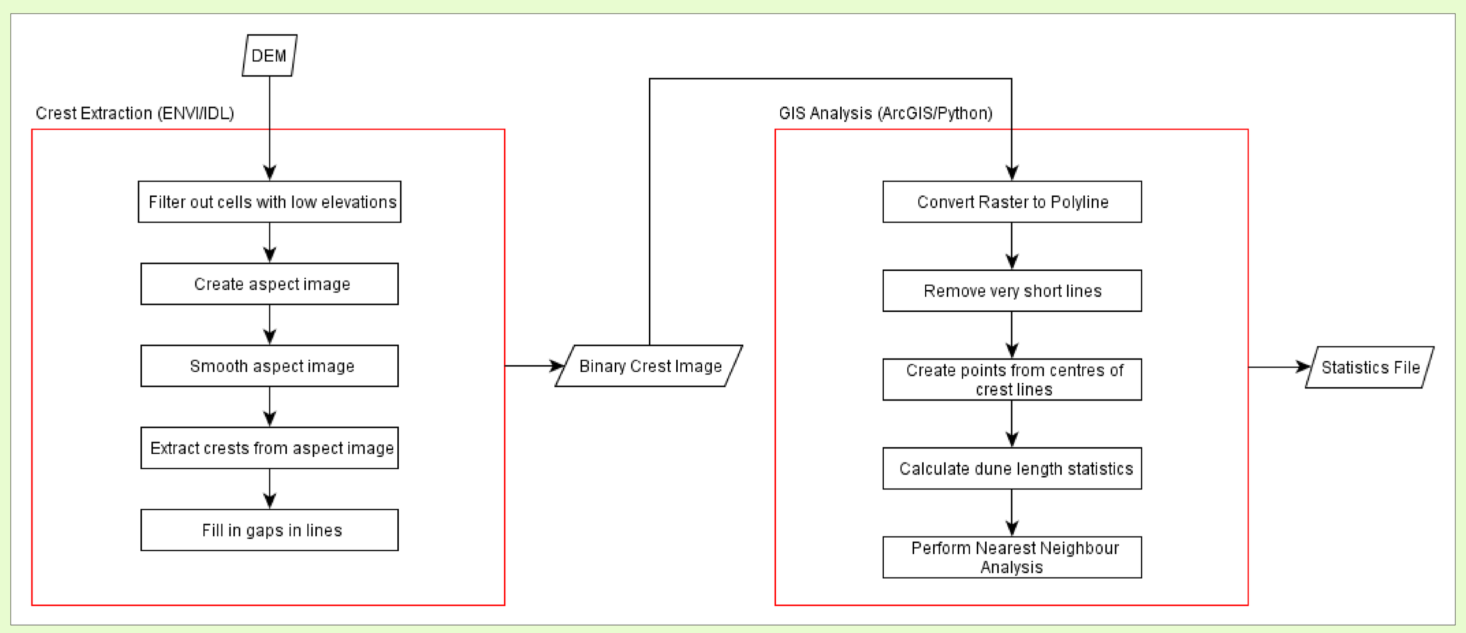

3. Modelling Surface Moisture

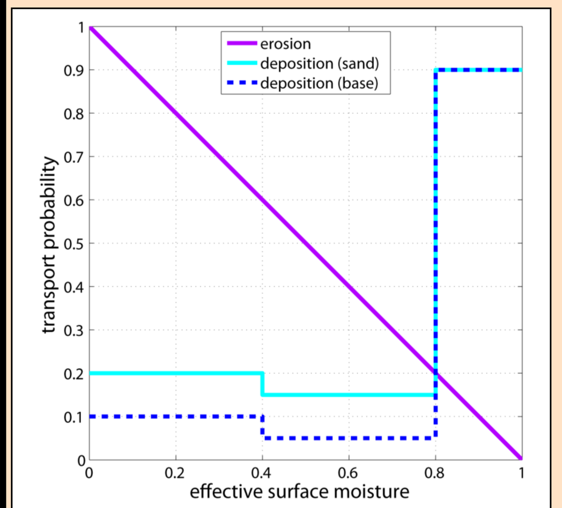

Fig. 3.1 Sediment erosion and deposition probabilities based on effective surface moisture and sediment presence.

Surface moisture is a key controlling factor for sediment transport in aeolian environments. Its presence raises the shear velocity threshold required to entrain sediment (Namikas and Sherman, 1995), but also forms a harder surface when the ground is partially saturated, over which grain rebound is more elastic (McKenna Neuman and Scott, 1998). We model this behaviour by varying stochastic transport in the DECAL algorithm according to effective surface moisture (Fig. 3.1). The response of surface moisture to sedimentation is included through a feedback function (Fig. 3.2). Surface moisture is updated every ten iterations, with net erosion exposing wetter underlying substrate, and net deposition drying the surface. Modelled behaviour mimics anticipated real-world observations, but further work is required to implement other hydrological aspects.

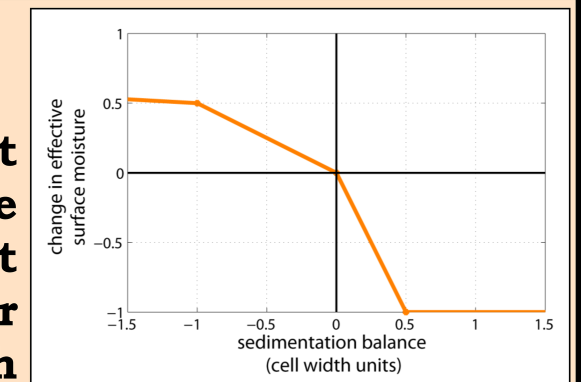

Fig. 3.2 Surface moisture and sedimentation relationship

4. Surface Moisture Influence on Pattern Development

The influence of surface moisture can be seen in coastal areas such as Guerrero Negro, Mexico (e.g. Inman *et al.*, 1966), or continental dune fields such as White Sands, USA. At White Sands, both Rachal and Dugas (2009) and Ewing and Kocurek (2010) suggest that increased moisture, either temporally due to an elevated water table during periods of increased precipitation or spatially in the central part of the dune field, is responsible for disorganisation with respect to dune patterns. We simulate the influence of surface moisture part way through the development of a barchan dune field using metrics calculated through the methods in Section 2.

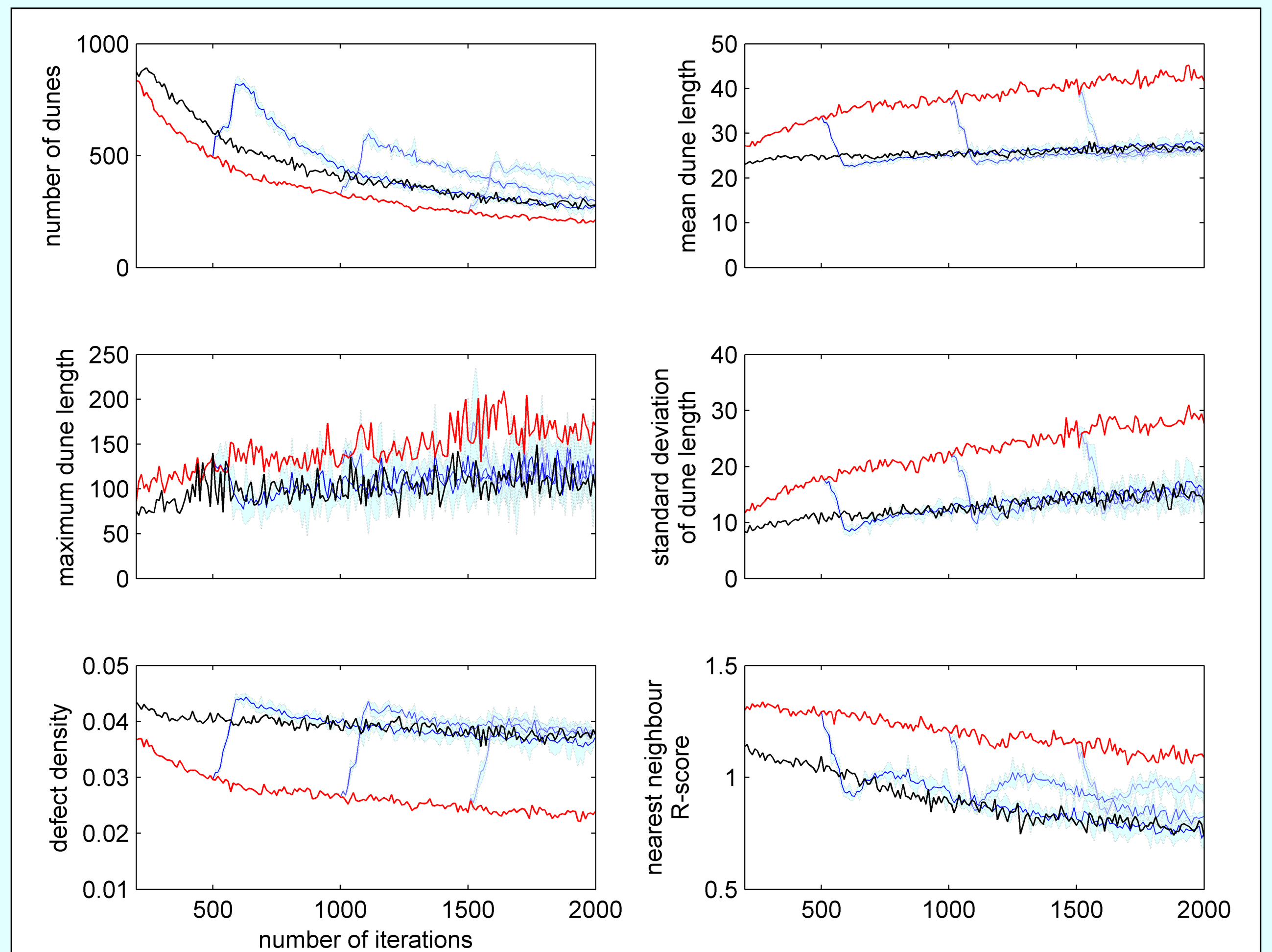

Fig. 4.1 Metric trends for 1000 x 1000 grid under dry (red line) or moist (black line) conditions. Blue lines indicate trends when surface moisture influences are applied part way through a simulation. Shaded area indicates twice standard deviation for behaviour of ten simulations.

Simulations indicate an increase in dune number and defect density immediately following the increase in surface moisture. Moisture limits the availability of sediment, reducing the potential for dune-dune interactions, as observed by Ewing and Kocurek (2010) at White Sands.

The nearest neighbour R-score also reduces with the introduction of surface moisture into the simulated environment, further suggesting a move towards disorder.

Dune length and defect density characteristics appear to be predominately controlled by moisture feedback rather than simulation duration.

5. Further Research

The crest extraction method also works on real-world DEMs collected through LiDAR and InSAR surveys which opens a number of possibilities for analysis of the self-organisation of large dunefields (such as White Sands) over long timescales. Automation increases the efficiency of analysing larger areas, thus greatly increasing the statistical accuracy of the results and allowing further statistics to be calculated which were previously invalid due to low sample sizes. Examples include analysis of histogram shapes to determine how the number of dunes of different sizes changes as the dune field evolves, and extraction of dune areas and volumes as well as dune crest lengths.

This method works well on barchan dunes but further development is needed to improve crest extraction of more complex dune fields, particularly reducing crest fragmentation and improving point placement on asymmetric dunes. Work is underway to address these issues, but, as always, there is a trade-off between accuracy and computational efficiency.

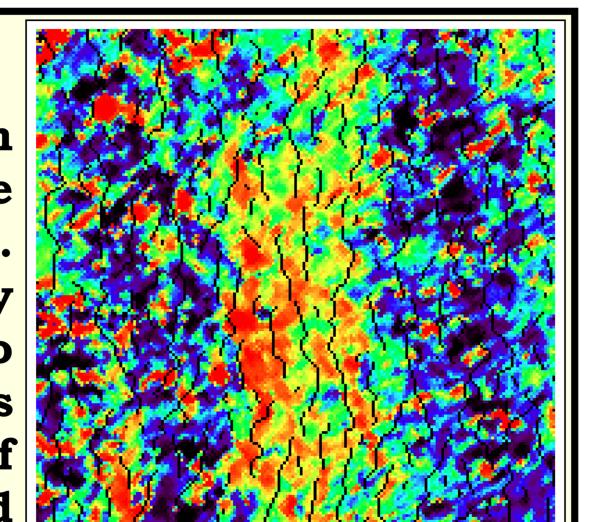

Fig. 5.1 Ubari Sand Sea, Libya; crest lines extracted from ASTER GDEM data

References

Ewing RC, Kocurek G. 2010. Aeolian dune interactions and dune-field pattern formation: White Sands Dune Field, New Mexico. *Sedimentology* 57: 1199-1219.
Ewing RC, Kocurek G, Lake LW. 2006. Pattern analysis of dune-field parameters. *Earth Surface Processes and Landforms* 31: 1176-91.
Inman DL, Ewing GC, Corliss JB. 1966. Coastal Sand Dunes of Guerrero Negro, Baja California, Mexico. *Geological Society of America Bulletin* 77: 787-802.
McKenna Neuman C, Scott MM. 1998. A wind tunnel study of the influence of pore water on aeolian sediment transport. *Journal of Arid Environments* 39: 403-419.
Namikas SL, Sherman DJ. 1995. A review of the effects of surface moisture content on aeolian sand transport. In: Desert Aeolian Processes (Ed. Tchakerian VP), Chapman and Hall, USA, 269-293.
Nield JM, Baas ACW. 2008. Investigating parabolic and nebkha dune formation using a cellular automaton modelling approach. *Earth Surface Processes and Landforms* 33: 724-740.
Rachal DM, Dugas DP. 2009. Historical dune pattern dynamics: White Sands Dune Field, New Mexico. *Physical Geography* 30: 64-78.
Wilkins DE, Ford RL. 2007. Nearest neighbour methods applied to dune field organisation: The Coral Pink Sand Dunes, Kane County, Utah, USA. *Geomorphology* 83: 48-57.

Simulations for this research were undertaken on the Iridis 3 High Performance Computing Cluster, University of Southampton